

Article

Experimental Study on the Mechanical Properties and Disintegration Resistance of Microbially Solidified Granite Residual Soil

Shihua Liang ¹, Xueli Xiao ¹, Caixing Fang ², Deluan Feng ^{1,*} and Yuxin Wang ¹

¹ School of Civil and Transportation Engineering, Guangdong University of Technology, Guangzhou 510006, China; shihua_l@gdut.edu.cn (S.L.); 2112009005@mail2.gdut.edu.cn (X.X.); 2112109097@mail2.gdut.edu.cn (Y.W.)

² Shenzhen Railway Investment Construction Group Co., Ltd., Shenzhen 518000, China; fangcaixing@shenzhenmc.com

* Correspondence: danniefung@gdut.edu.cn

Abstract: Microbially induced calcium carbonate (CaCO₃) precipitation (MICP) is an emerging soil-treatment method. To explore the effect of this technology on granite residual soil, this study investigated the effects of the mechanical properties and disintegration resistance of microbially cured granite residual soil under different moisture contents by conducting direct shear and disintegration tests. The curing mechanism was also discussed and analyzed. Results showed that MICP can be used as reinforcement for granite residual soil. Compared with those of untreated granite residual soil, the internal friction angle of MICP-treated granite residual soil increased by 10% under a moisture content of 30%, while its cohesion increased by 218%. The disintegration rate of the MICP-treated granite residual soil stabilized after a maintenance time of 5 days under different water contents. Therefore, we provide the explanation that the improvement of the shear strength and disintegration resistance of granite residual soil is due to CaCO₃ precipitation and the surface coating.

Keywords: microbially induced calcium carbonate precipitation; granite residual soil; moisture content; shear strength; disintegration test



Citation: Liang, S.; Xiao, X.; Fang, C.; Feng, D.; Wang, Y. Experimental Study on the Mechanical Properties and Disintegration Resistance of Microbially Solidified Granite Residual Soil. *Crystals* **2022**, *12*, 132. <https://doi.org/10.3390/cryst12020132>

Academic Editors: Changquan Calvin Sun and Ruikang Tang

Received: 17 November 2021

Accepted: 13 January 2022

Published: 18 January 2022

Publisher's Note: MDPI stays neutral with regard to jurisdictional claims in published maps and institutional affiliations.



Copyright: © 2022 by the authors. Licensee MDPI, Basel, Switzerland. This article is an open access article distributed under the terms and conditions of the Creative Commons Attribution (CC BY) license (<https://creativecommons.org/licenses/by/4.0/>).

1. Introduction

Granite residual soil is the product of the chemical and physical weathering of a parent rock, and it exhibits the characteristics and engineering properties of clayey and coarse-grained soils [1]. As a special soil, granite residual soil differs from general clayey and sandy soils, which are widely distributed in the coastal area of southeast China [2,3]. Although its engineering properties are good in its natural state, granite residual soil easily softens and disintegrates after being soaked in water, inducing the gradual damage caused by destabilization due to scouring of granite residual soil slope. Li et al. [3] determined that different initial moisture contents are important factors that influence the disintegration of granite residual soil. Given its poor engineering characteristics, such as being susceptible to softening and disintegration by water, granite residual soil is prone to geological hazards, including landslides. To enhance the strength and water stability of soil, granite residual soil must be solidified and improved in engineering construction. Chemical improvement methods are commonly used to reinforce granite residual soil in actual engineering construction; these methods include mixing appropriate amounts of lime [4,5] or cement [5,6] into the soil to cause a series of physical and chemical reactions that will cement soil particles, improving the strength and water stability of granite residual soil. These chemical reinforcement techniques are highly predisposed to causing unsustainable damage to the local environment. Therefore, exploring environmentally friendly soil consolidation techniques is urgent to improve the undesirable engineering properties of granite residual soil.

Microbially induced calcium carbonate precipitation (MICP) refers to the application of microbial metabolism to produce urease, which hydrolyzes urea to generate NH_4^+ and CO_3^{2-} . Then, CO_3^{2-} combines with Ca^{2+} in the surrounding environment to form CaCO_3 crystal precipitation, cementing sand particles and effectively improving the mechanical properties of soil [7–11]—see Figure 1. At present, MICP is mostly applied to improve the engineering properties of sandy soil in porous media [12–14]; however, residual soil is fundamentally different from sandy soil in terms of particle gradation, microstructure, and pore characteristics. The use of conventional circulation grouting is unsuitable for soil with small pores. For soft soil with low porosity and residual soil, the curing method of mixing bacterial and nutrient solutions to produce samples is more suitable. Tiwari et al. [15] performed MICP treatment on bentonite via mixing and found that the unconfined compressive strength of the MICP-treated specimens increased by more than 205% compared with that of the untreated specimens. Xiao et al. [16] reported that the preparation of soft soil treated with MICP via direct mixing can promote the formation of CaCO_3 crystals. Ou et al. [17] used a combination of microbial and quicklime consolidation on overwet bauxite tailings clay and found that biochemical consolidation made the soil more compact. Vail et al. [18] studied the desiccation cracking behavior of compacted calcium bentonite soil by using the MICP mixing method. They determined that MICP reactions effectively delay crack initiation and remediate desiccation cracking, as reflected by the decrease in the geometrical descriptors of the crack pattern, such as surface crack ratio. Soil improvement using MICP is a novel and innovative technique compared with the conventional methods that have been in use for environmental applications [19]. However, the main problem induced by MICP is the release of ammonia during the cementation process, imposing a negative impact on the ecological environment once excessive ammonia has been produced [20], approximately according to the following Equation (1). Studies have shown that the use of low-pH MICP [21,22], struvite precipitation [23], and calcium phosphate biocement [22,24] is more effective in reducing the amount of ammonia produced. More research on ammonium ion-removal methods is needed in the future to promote the application of MICP [25].

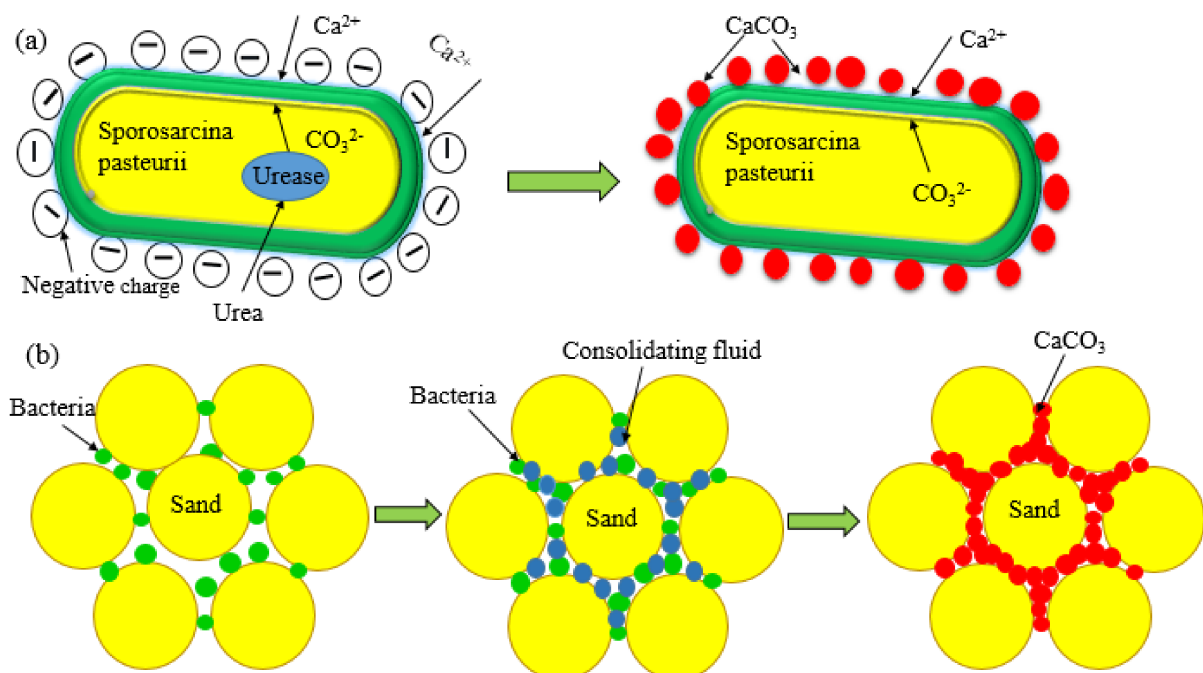


Figure 1. Schematic diagram of microbial solidified sand.

Modifying low-permeability clay soil via MICP mixing and sample making is practical; however, granite residual soil is fundamentally different from clay and silt in the aspects of particle size distribution, microstructure and pore characteristics. It also has significant softening and disintegration characteristics when subjected to water. Granite residual soil is widely distributed in southern China [19]. Due to its special causes, there are a large number of primary cracks in the soil, and it is easy to cause the development of secondary cracks when the external environmental factors change. The nature of the soil is uneven, and it is easy to soften and disintegrate in water [26]. Soil disintegration refers to the phenomenon of soil rupture and dispersion due to water immersion. This is an irreversible physical process in which the cementation between soil particles is lost under the action of water immersion, and the soil structure collapses due to the stress concentration caused by the repulsion between particles exceeding the suction. When the granite residual soil slope makes contact with water, it will destroy the cementation force in the soil, reduce the strength of the soil, and easily induce geological disasters such as landslide instability [27,28]. MICP is often used to improve the compressive strength of sand at first, and a few studies are used in silt with relatively small particle size and pore throat size, but the purpose is to improve the bearing performance of foundation soil. The engineering performance of granite residual soil is good under natural conditions, but it is easy to soften and collapse in water, resulting in the instability of granite residual soil slope. In the current study, the feasibility of MICP technology in curing granite residual soil was initially demonstrated by performing direct shear and disintegration tests on granite residual soil samples before and after MICP treatment. The mechanism of MICP action when curing granite residual soil was initially discussed by comparing the samples before and after MICP treatment and scanning electron microscopy (SEM) test analysis. This paper provides a reference for the application of calcium carbonate crystals in granite residual soils.

2. Materials and Methods

2.1. Soil

The test sample was obtained from granite residual soil in the eastern part of Guangzhou City, China. Its basic physical properties were as follows: moisture content (32%), wet density (1.76 g/cm^3), liquid limit (41.2%), and plasticity index (17.76). Results of chemical analysis performed using an Energy Dispersive X-ray Fluorescence (XRF) spectrometer (PANalytical B.V., Almelo, The Netherlands) reveal that the slope soil majorly consists of Na_2O , Al_2O_3 , Fe_2O_3 , Cl , CaO , and K_2O of 58.79%, 20.33%, 3.00%, 1.72%, and 1.01%, respectively. The PH of the granite residual soil is 6.62. The granite residual soil sample was dried, and then the drying soil sample was placed on a rubber plate and crushed with a wooden mill. The dispersed soil sample was passed through a 2 mm sieve. A sufficient amount of sieved, drying soil sample was obtained and set aside. The particle gradation curve of granite residual soil after sieving is shown in Figure 2, where coefficient of uniformity $C_u = 5.2$ and median particle diameter $D_{50} = 0.2 \text{ mm}$. Soil particles are relatively uniform and poorly graded.

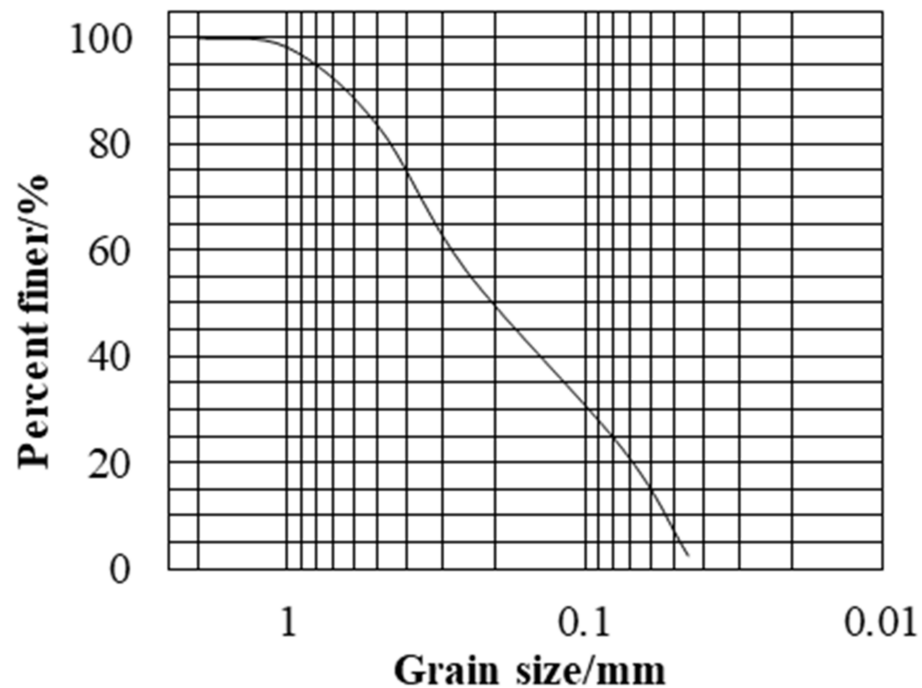


Figure 2. Particle grading curve.

2.2. Bacterial and Nutrient Solutions

The *Bacillus pasteurii* (No. DSM33) which was purchased from DSM (the Netherlands) was freeze-dried. The composition of the liquid medium was as follows: yeast (20 g/L), ammonium sulfate (10 g/L), and sodium hydroxide (2 g/L). The composition of the nutrient solution was 111 g/L of calcium chloride and 60.06 g/L of urea. The average urease activity in this pilot study was 13.3 $\mu\text{mol}/\text{min}/\text{mL}$ and the average OD_{600} of bacteria was 1.749.

2.3. Sample Preparation

This test used the method of mixing and making samples, a dry density of 1.5 g/cm^3 and an initial pore ratio of 0.7 were selected to ensure that the dry density of each specimen was the same. Specimen preparation without MICP curing: three water contents (10%, 20%, and 30%) were selected, and the calculated amount of required water was mixed with soil. Specimen preparation for MICP curing of granite residual soil: Equal volumes of bacterial and nutrient solutions were first mixed to produce a microbial curing agent. This agent was mixed into the drying soil instead of water at the corresponding moisture content and mixed thoroughly. The mass of wet soil required to prepare the specimen was determined in accordance with the dry density required for the test by using Equation (2):

$$m = (1 + 0.01\omega) \cdot \rho_d \cdot V, \quad (2)$$

where:

m —the mass of wet soil required to prepare the specimen (g);
 ρ_d —the dry density required to prepare the specimen (g/cm^3);
 V —the volume of the specimen (cm^3);
 ω —water content (%).

The wet soil was poured into a ring-knife sample maker (inner diameter 61.8 mm, height 20 mm), and the sample was pressed. The sample was removed and kept in a curing box with a constant temperature of 25 °C and a humidity of 95% for 3, 5, and 7 days. The sample which was cured for 5 days was used for the direct shear and disintegration tests. The samples cured for 3 days and 7 days were used for the disintegration test. The water contents of the specimens after maintenance are provided in Table 1. The water content of

MICP was basically the same before and after curing. In the current study, 10%, 20%, and 30% water contents represented the contents of the solution (i.e., water or microbial curing agent) added during the preparation of the specimens as a percentage of the drying soil and the initial water content.

Table 1. Moisture content of the samples after curing.

Curing Time (d)	Water Content (%)					
	Water			Micp		
	10	20	30	10	20	30
3	10.7	20.7	27.1	10.2	20.2	27
5	10.6	20.5	27.2	10.4	21	27.2
7	10.1	21.2	27.8	10.8	19.9	27.1

2.4. Direct Shear Test

The direct fast shear test and the ZJ strain controlled direct shear apparatus (Nanjing Nantucket Instruments & Equipment Co., Nanjing, China) were used in this study—see Figure 3. This device uses a stepper motor, continuous variable, and can input any speed within the range of the test protocol for shearing. Furthermore, the device has a shear box with a diameter of 61.8 mm (upper and lower shear box heights of 10 and 10 mm, respectively). The shear displacement and vertical deformation of the sample were measured using two percentage meters. Percentage meter readings were accurate to 0.01 mm. Each group used four specimens that were under vertical pressures of 100, 200, 300, and 400 kPa. Then, horizontal shear force was applied to the shear. The shear rate was set as 0.8 mm/min. Data were recorded every 15 s. The rotation of the percentage meter on the force ring was observed after pressure. The percentage meter pointer was no longer facing forward or the pointer began to regress when the peak of the force ring readings was reached; that is, the specimen was damaged. Shear-to-shear displacement of the 6 mm stop test was continued. The angle of internal friction φ and cohesion c were determined as indicators of the shear strength of the soil in accordance with Coulomb's law. Each group was conducted according to the relevant soil test specification [29].

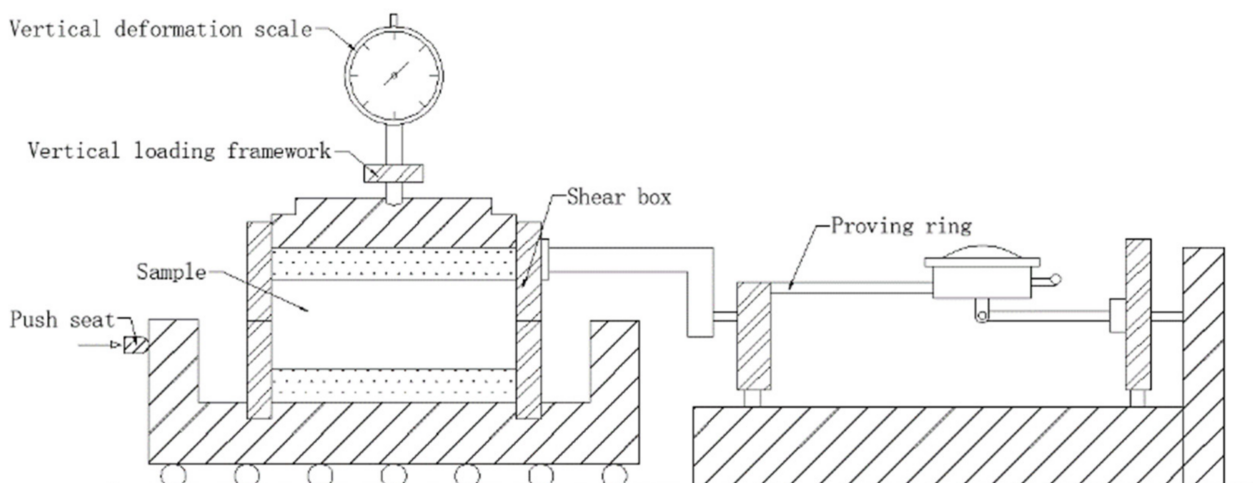


Figure 3. Shear test apparatus.

2.5. Disintegration Test

This test used the mass method to study the disintegration characteristics of granite residual soil [30–32]. The disintegration test apparatus is shown in Figure 4. Each group used three specimens. The ring-knife specimens were placed lightly on a metal wire mesh (10 cm × 10 cm), and the specimens and the wire mesh were completely submerged into

deionized water in a glass box, which was placed under a balance. As disintegration proceeded, the disintegrated soil sample fell to the bottom of the glass box and the balance reading decreased. The readings were converted to obtain the disintegration rate at each time. The conversion relationship is shown in Equation (3).

$$P = \frac{D_0 - D_t}{D_0 - D'} \times 100\% \quad (3)$$

where:

$P(t)$ —the cumulative amount of disintegration of a specimen at moment t (%);

D' —the initial reading of the balance (i.e., the balance reading when the empty wire mesh is immersed into water) (g);

D_0 —the balance reading in the beginning of the test (g);

D_t —the balance reading at moment t (g).

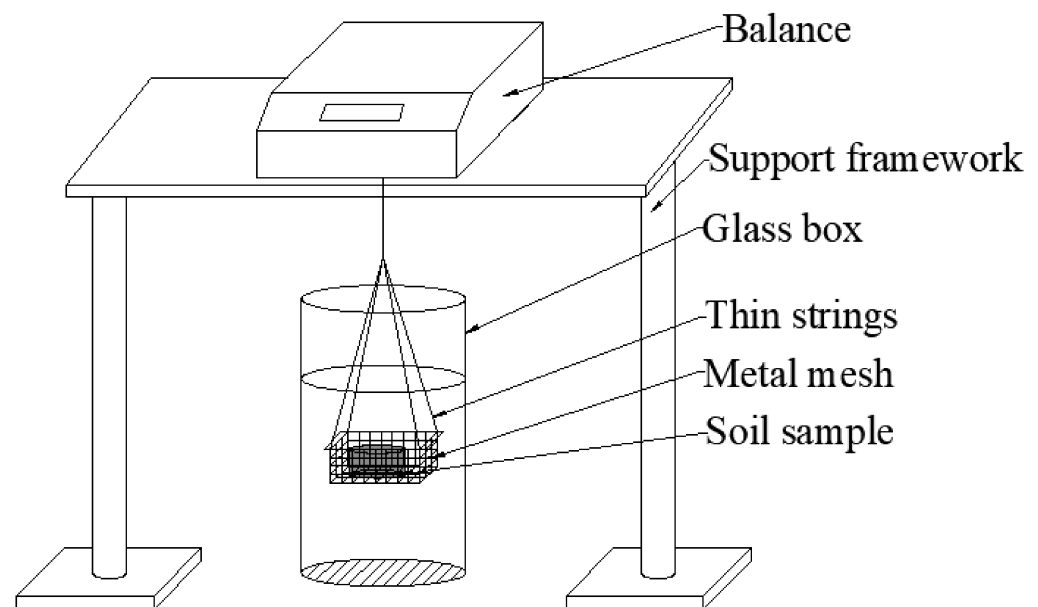


Figure 4. Disintegration test apparatus.

2.6. SEM and XRD Experiment

At the end of the experiments, the verification of the sample was performed via SEM and XRD analyses. The crushed sample underwent examination of SEM (SUPRATM 55, Germany) after being gold-coated. The microscopic morphology of the sample was observed by SEM. Afterwards, the powder was sampled for XRD analysis (Bruker, Berlin, Germany). Mineral composition was determined with XRD.

2.7. Determination of Water-Stable Agglomerate Content

In accordance with the wet sieve method of determination, 500 g of dry specimen was obtained and a set of sieves with meshes of 2, 1, 0.5, and 0.25 mm was used. A specimen was placed on the top layer of the 2 mm sieve, and then the set of sieves was placed slowly in a cylinder with a sufficient amount of deionized water and oscillated for 2 min. The set of sieves was removed, retaining an appropriate amount of deionized water to collect the agglomerates at all sieve levels. The agglomerates were dried at all levels and weighed. The mass fraction of the agglomerates was calculated at all levels.

3. Results

3.1. Analysis of the Shear Strength of Granite Residual Soil before and after MICP Curing

The shear stress and shear displacement curves of granite residual soil under different vertical loads are shown in Figure 5. On the basis of the image characteristics of the shear stress and shear displacement curves of each group, the shear strengths of granite residual soil before and after MICP curing under different water contents were obtained and are provided in Table 2.

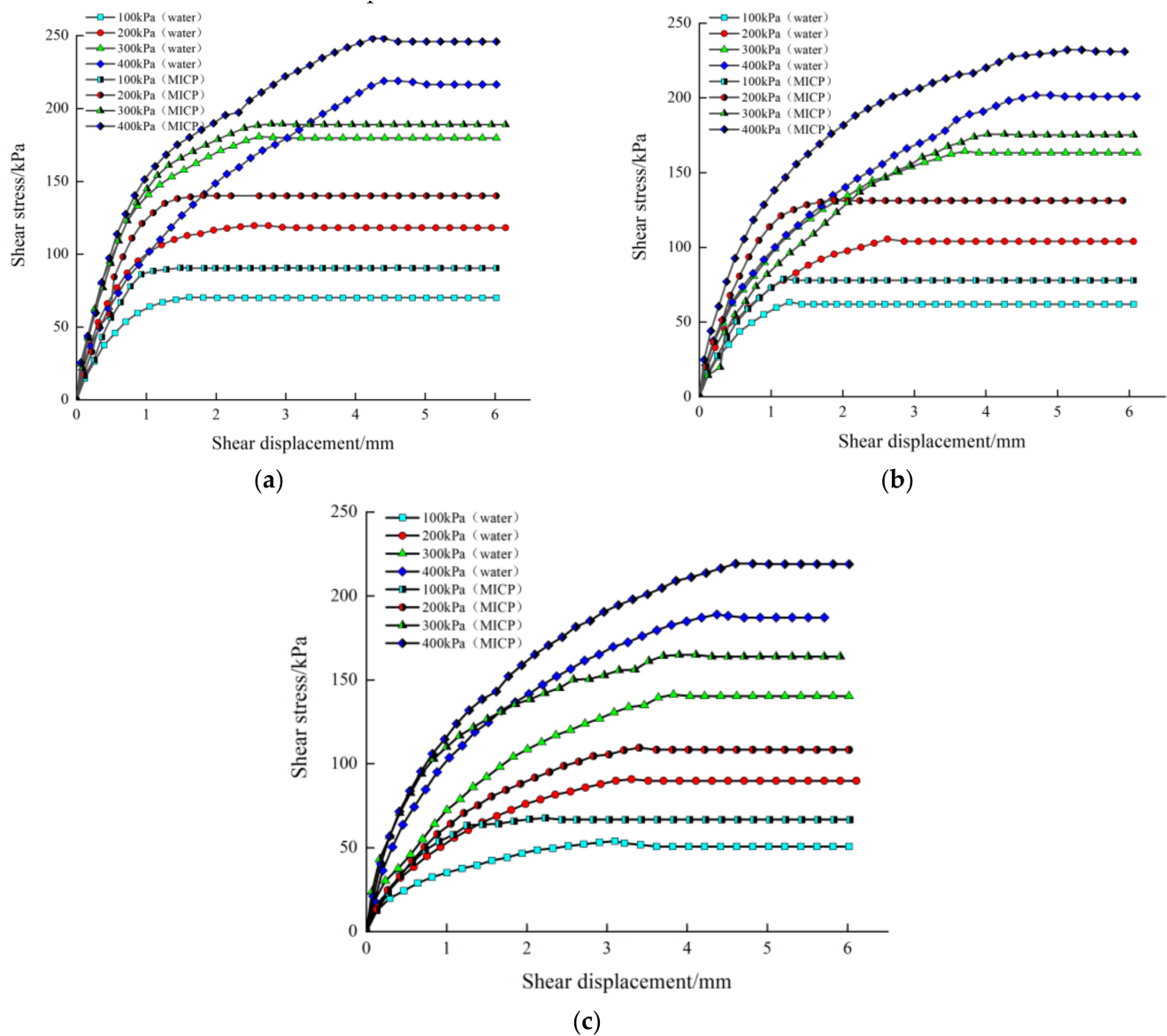


Figure 5. Curve of the shear stress and shear displacement of a specimen: (a) 10%, (b) 20%, and (c) 30% water contents.

Table 2. Shear strength of granite residual soil before and after MICP curing under different moisture contents.

	Water Content (%)	Vertical Pressure (kPa)			
		100	200	300	400
Water	10	70.46	119.64	180.75	218.92
	20	63.31	105.51	164.23	201.85
	30	53.12	90.83	141.30	189.01
MICP	10	90.65	140.27	189.42	248.09
	20	78.08	131.94	175.74	232.13
	30	67.71	109.55	164.97	219.28

On the basis of the shear strength under four different vertical pressures, namely, 100, 200, 300, and 400 kPa (Table 2), the relationship curves between shear strength and vertical pressure were plotted, as shown in Figure 6. Then, linear fitting was performed to obtain the internal friction angle φ and cohesive force c before and after MICP curing under different water contents (Table 3).

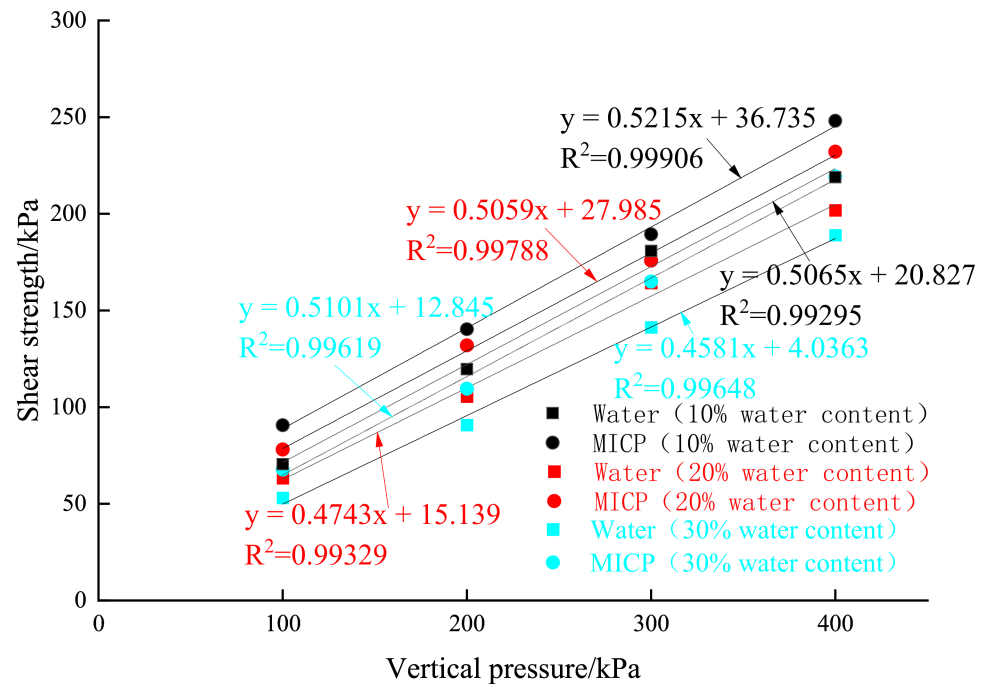


Figure 6. Curve of the shear strength and vertical pressure of granite residual soil under different water contents.

Table 3. Internal friction angle and cohesion of granite residual soil under different water contents.

Water Content (%)	Internal Friction Angle (°)		Cohesion (kPa)	
	Water	MICP	Water	MICP
10	26.9	27.5	20.8	36.7
20	25.4	26.8	15.1	27.9
30	24.6	27.0	4.0	12.9

As indicated in Table 2, the shear strength of granite residual soil under different vertical pressures decreased with an increase in water content. Under the condition that water content remained constant, shear strength increased with an increase in vertical pressure. As shown in Table 3, the internal friction angle and cohesion of granite residual

soil decreased with an increase in water content. Cohesion force c decreased more than the internal friction angle φ . The cohesion force of granite residual soil with 20% and 30% water contents decreased by 27% and 80% more than the 10% water content, while the internal friction angle decreased by only 5.5% and 8.4%, respectively.

Figure 6 shows that the shear strength of the MICP-cured granite residual soil under different moisture contents and vertical pressures was greater than that of the uncured specimen. The increase in shear strength was primarily reflected in the increase in internal friction angle and cohesion. The increase in cohesion was greater than the increase in internal friction angle. Compared with that of the uncured granite residual soil, internal friction angle increased by 3%, 6%, and 10% after curing under the moisture contents of 10%, 20%, and 30%, respectively. The changes in internal friction angle of granite residual soil before and after MICP curing were within the range of 0.7–2.4°; these values were insignificant. Therefore, the effect of curing granite residual soil with MICP on the internal friction angle was minimal.

The improvement of cohesion after MICP curing was more significant compared with that of internal friction angle. Under the water contents of 10%, 20%, and 30%, the cohesion of the MICP-cured granite residual soil was increased by 76%, 85%, and 218%, respectively, compared with that of granite residual soil without MICP treatment.

3.2. Disintegration Test

The X-ray diffraction (XRD) pattern in Figure 7 shows that granite residual soil contains kaolinite minerals, which exhibit solubility and swelling in water [33], causing soil to soften and disintegrate easily in water.

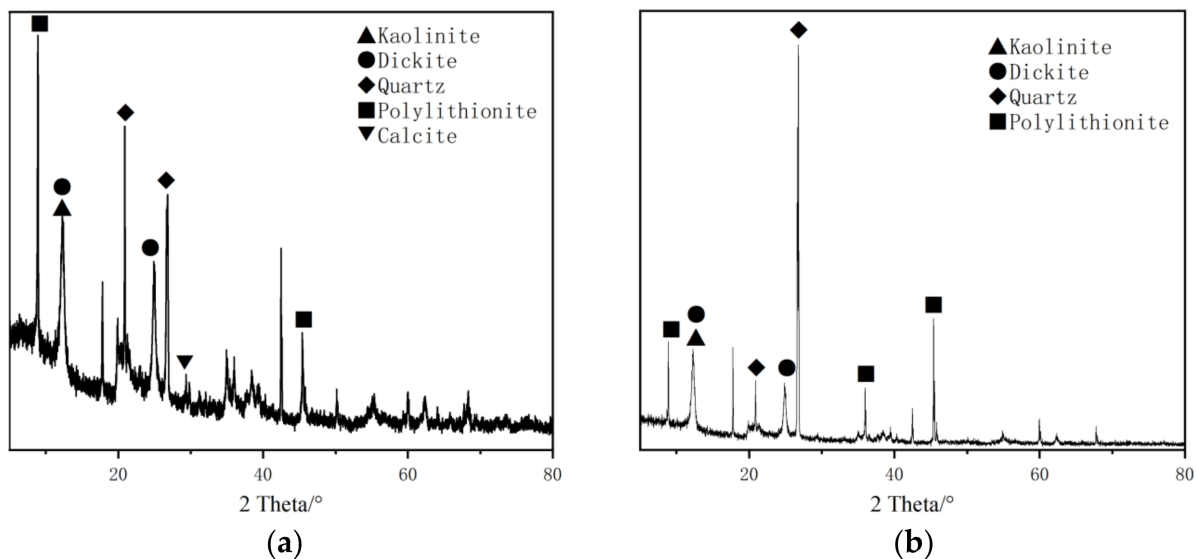


Figure 7. XRD pattern of granite residual soil: (a) MICP and (b) water.

Figure 8 presents the disintegration curves of granite residual soil before and after MICP-curing under different water contents with maintenance times of 3, 5, and 7 days. Untreated granite residual soil disintegrated after 3, 5, and 7 days under three different water contents. In particular, granite residual soil with 10% and 20% water contents completely disintegrated within a short time, while granite residual soil with 30% water content partially disintegrated. This finding is consistent with the conclusion drawn by Li [3] when he studied the effect of water content on the disintegration characteristics of granite residual soil.

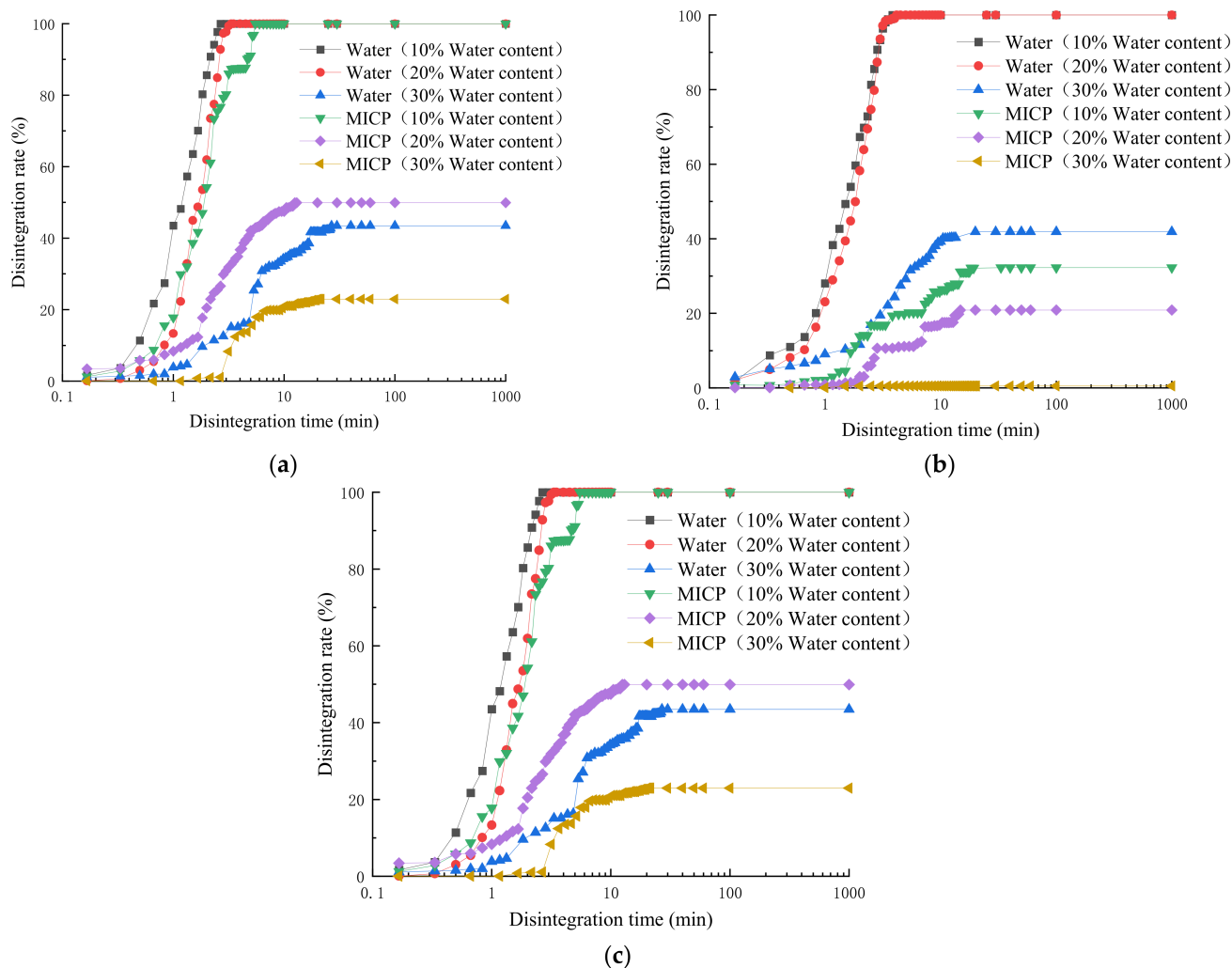


Figure 8. Disintegration curve: (a) Conservation of 3 days, (b) 5 days, and (c) 7 days.

Granite residual soil cured via MICP with 10% water content disintegrated completely within a short time at a maintenance period of 3 days. Meanwhile, granite residual soil cured via MICP with 20% and 30% water contents achieved a stable state after partial disintegration. Granite residual soil cured via MICP with 10% water content exhibited incomplete disintegration at maintenance periods of 5 days and 7 days. Meanwhile, granite residual soil cured via MICP with 30% water content nearly did not disintegrate, with disintegration rates of only 0.5% and 0.36% after 48 h of observation. MICP curing produced CaCO_3 precipitation, which can fill gaps between soil particles and reduce pores on the soil surface, preventing water from entering the interior of the soil and effectively improving the poor engineering characteristics of granite residual soil, which is prone to disintegration when exposed to water. In addition, the disintegration resistance of granite residual soil is related to the quantity and quality of the water-stable agglomerates of its soil structure [33]; the higher the number of water-stable agglomerates and the larger the particle size, the better the disintegration resistance of soil. The content of water-stable agglomerates is positively correlated with CaCO_3 content. Figures 9 and 10 show that a small amount of CaCO_3 crystals generated from MICP-treated granite residual soil exist in the form of CaCO_3 . These crystals are beneficial for the formation of water-stable agglomerates in soil, making soil less likely to disintegrate and crack in water, and thus, improving the disintegration resistance of granite residual soil.

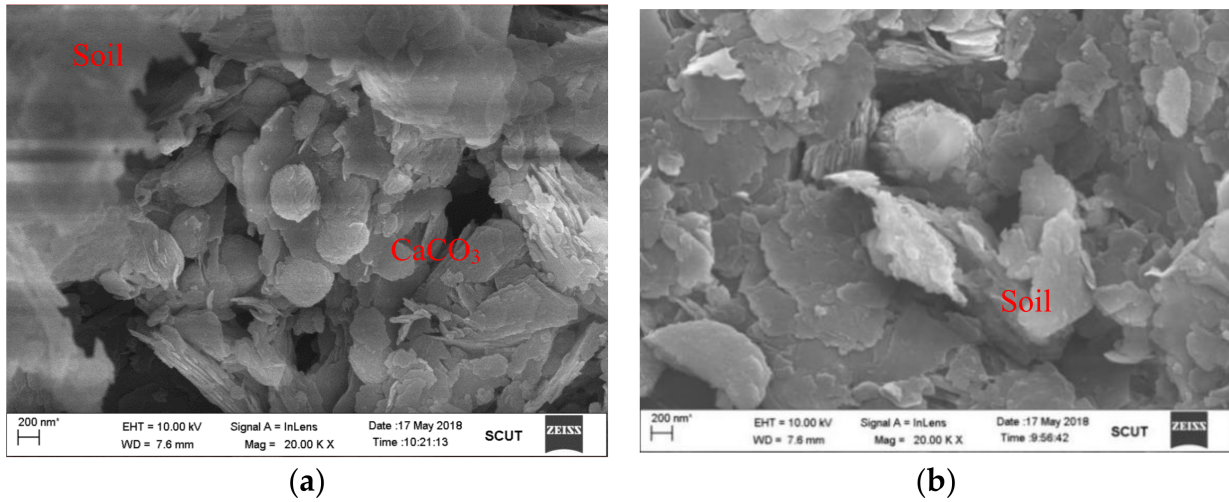


Figure 9. SEM image of granite residual soil: (a) MICP and (b) water.

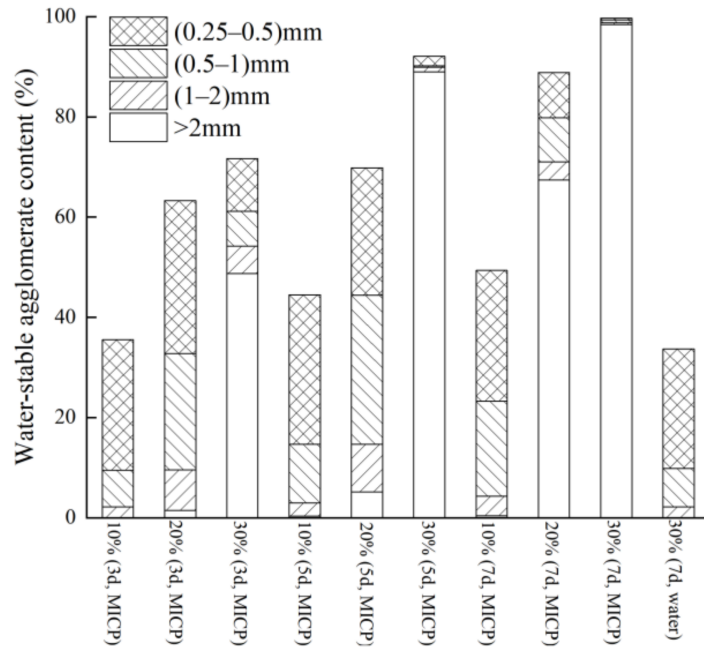


Figure 10. Water-stable agglomerate content of the samples.

The effect of MICP curing on granite residual soil under 30% water content was better than that under 10% and 20% water contents when maintenance time was 3, 5, and 7 days because of the following two reasons. First, granite residual soil under high water content was more resistant to disintegration than granite residual soil under low water content. Second, more bacterial and nutrient solutions were added under 30% water content than under 10% and 20% water contents, producing more CaCO₃ and a better curing effect. Figure 6 shows the variation in disintegration rate of the MICP-cured granite residual soil with maintenance time. Disintegration rate decreased with an increase in maintenance time and stabilized after 5 days. According to the test results and the reinforcement mechanism of MICP, the MICP reinforcement technology has good application prospects in the anti-erosion prevention and control of granite residual soil. The reaction of MICP was essentially completed after 5 days.

3.3. SEM and XRD

Granite residual soil before and after MICP curing was collected for the SEM and XRD tests. Figure 8 shows that the major components of granite remnants are kaolinite, dickite, and quartz. Meanwhile, CaCO_3 is found in the mineral composition of the MICP-cured granite remnants. Figure 9 illustrates that MICP partially filled the pores between soil particles, cemented soil particles together, effectively enhanced shear strength, and improved the disintegration characteristics of granite residual soil. The increase in the internal friction angle is attributed to MICP on the surface of soil particles, filling the pores and reducing the porosity of soil. The deposition of CaCO_3 precipitates onto the surface of soil particles increases surface roughness, and consequently, the frictional properties of the surface of soil particles. Sivakumar and Ashkan agree that the precipitation of calcium carbonate crystals can increase the roughness of soil particles, which is an important factor in the shear strength of soils [34,35]. The most important reason for the increase in cohesion is the microbially induced production of CaCO_3 colloidal soil particles. This process improves the integrity of soil, and thus, increases the cohesion of granite residual soil. The cohesive force of specimens with high water content was significantly reduced compared with that of specimens with low water content because of the softening effect of water on the mucilage of granite residual soil. When MICP curing was performed with the same contents of bacterial and nutrient solutions, specimens with high water content produced relatively more CaCO_3 precipitation, which exerted a certain cementing effect on the softened mucilage. Therefore, the effect of MICP curing on granite residual soil was relatively better under high water content. The amount of CaCO_3 precipitation observed in the SEM test images was not considerably relative to the coarse-grained content of granite residual soil. Thus, MICP treatment is presumed to have a greater cementing effect than filling effect on granite residual soil. Hence, the improvement in cohesion was greater than that in the internal friction angle.

3.4. Water-Stable Agglomerate Content

In soil science, the content of water-stable agglomerates is the best indicator of soil erosion resistance. The higher the content of water-stable agglomerates (>0.25 mm), the stronger the erosion resistance of soil. Figure 10 presents the water-stable agglomerate content of the specimens before and after MICP curing. The content of the specimens that did not undergo MICP curing is basically the same, and thus, only one group is listed. As shown in Figure 10, the content of water-stable agglomerates (>0.25 mm) of granite residual soil after MICP curing increased with an increase in maintenance time and water content. Moreover, the content of agglomerates with a particle size of >2 mm gradually increased. This finding is consistent with the variation pattern of disintegration rate with different maintenance periods after the MICP curing of granite residual soil under different water contents. As shown in Figure 11, a white overlay was observed on the surface of granite residual soil after 5 days of maintenance. This finding is similar to that of Cardoso [36] in her study on MICP-cured clay with a uniform overlay on the surface. However, the nature of this overlay requires further in-depth investigation. After comparing the samples before and after MICP treatment, the improvement in the shear strength and disintegration resistance of granite residual soil may be attributed to a combination of CaCO_3 crystals' precipitation and the surface coating.

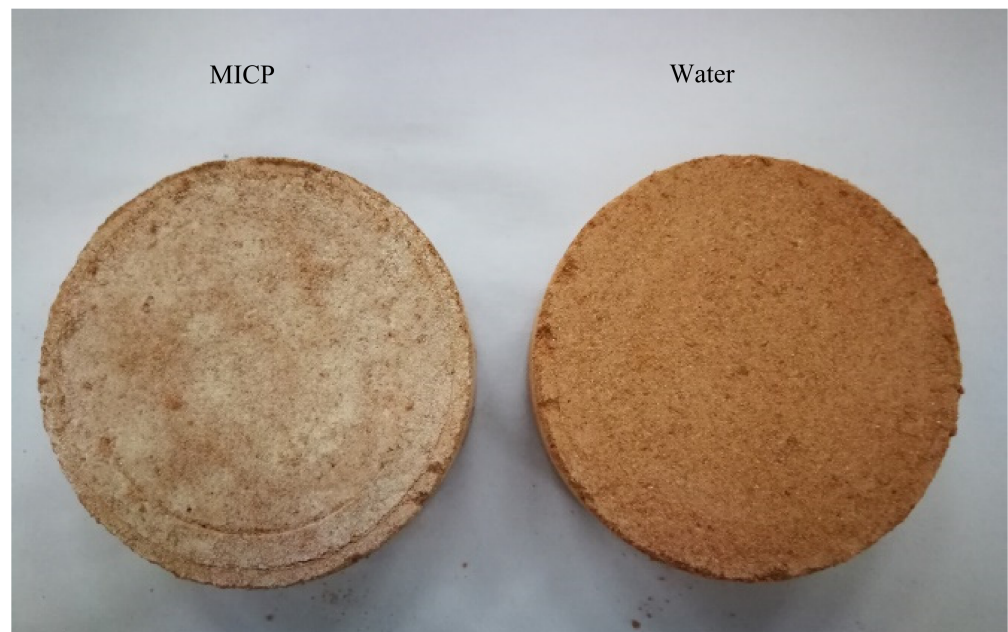


Figure 11. Granite residual soil samples.

4. Conclusions

- (1) The shear strength of granite residual soil decreases with an increase in water content. The cohesion and internal friction angle of its shear strength index also decrease with an increase in water content, and the effect of water content on internal friction angle is smaller compared with that of cohesion;
- (2) The shear strength of MICP-cured granite residual soil under three moisture contents (10%, 20%, and 30%) and vertical pressures of 100, 200, 300, and 400 kPa. The effect of MICP curing on cohesion was more significant than that on internal friction angle;
- (3) By combining the two shear strength indicators of internal friction angle and cohesion, the MICP curing of granite residual soil is relatively optimal when the water content of granite residual soil is 30%;
- (4) MICP technology can effectively improve the poor engineering characteristics of granite residual soil, which is prone to disintegration by water. The disintegration rate of MICP-cured granite residual soil decreases with increasing maintenance time and stabilizes after 5 days;
- (5) The improvement in shear strength and disintegration resistance of granite residual soil after treatment with MICP may be attributed to CaCO_3 precipitation and surface coating.

Author Contributions: Conceptualization, S.L.; Writing, D.F.; Formal analysis, C.F.; Data curation, X.X.; Supervision, Y.W. All authors have read and agreed to the published version of the manuscript.

Funding: This research was funded by the National Natural Science Foundation of China (grant number 52078142) and the Science and Technology Program of Guangzhou, China (grant number 202002030194).

Data Availability Statement: The data used to support the findings of this study are included within the article.

Conflicts of Interest: The authors declare no conflict of interest.

References

1. Zhai, Q.; Rahardjo, H.; Satyanaga, A. Variability in unsaturated hydraulic properties of residual soil in Singapore. *Eng. Geol.* **2016**, *209*, 21–29. [[CrossRef](#)]
2. Pan, Y.-L.; Jian, W.-X.; Li, L.-J.; Lin, Y.-Q.; Tian, P.-F. A study on the rainfall infiltration of granite residual soil slope with an improved Green-Ampt model. *Rock Soil Mech.* **2020**, *41*, 2685–2692.
3. Li, C.S.; Kong, L.W.; Shu, R.J.; An, R.; Zhang, X.W. Disintegration characteristics in granite residual soil and their relationship with the collapsing gully in South China. *Open Geosci.* **2020**, *12*, 1116–1126. [[CrossRef](#)]
4. Sun, Y.L.; Tang, L.S.; Wang, Y.X.; Xie, Z.X. Assessment of strength development in granite residual soil admixed coastal sludge. *Fresenius Environ. Bull.* **2021**, *30*, 758–770.
5. Cristelo, N.; Glendinning, S.; Miranda, T.; Oliveira, D.; Silva, R. Soil stabilisation using alkaline activation of fly ash for self compacting rammed earth construction. *Constr. Build. Mater.* **2012**, *36*, 727–735. [[CrossRef](#)]
6. Chew, S.H.; Kamruzzaman, A.H.M.; Lee, F.H. Physicochemical and engineering behavior of cement treated clays. *J. Geotech. Geoenviron. Eng.* **2004**, *130*, 696–706. [[CrossRef](#)]
7. Sun, X.H.; Miao, L.C.; Chen, R.F. Effects of Different Clay's Percentages on Improvement of Sand-Clay Mixtures with Microbially Induced Calcite Precipitation. *Geomicrobiol. J.* **2019**, *36*, 810–818. [[CrossRef](#)]
8. Arpajirakul, S.; Pungrasmi, W.; Likitlersuang, S. Efficiency of microbially-induced calcite precipitation in natural clays for ground improvement. *Constr. Build. Mater.* **2021**, *282*, 11. [[CrossRef](#)]
9. Han, L.; Li, J.; Xue, Q.; Che, Z.; Zhou, Y.; Poon, C.S. Bacterial-induced mineralization (BIM) for soil solidification and heavy metal stabilization: A critical review. *Sci. Total Environ.* **2020**, *746*, 140967. [[CrossRef](#)]
10. Rahman, M.M.; Hora, R.N.; Ahenkorah, I.; Beecham, S.; Karim, M.R.; Iqbal, A. State-of-the-Art Review of Microbial-Induced Calcite Precipitation and Its Sustainability in Engineering Applications. *Sustainability* **2020**, *12*, 41. [[CrossRef](#)]
11. Gebru, K.A.; Kidanemariam, T.G.; Gebretinsae, H.K. Bio-cement production using microbially induced calcite precipitation (MICP) method: A review. *Chem. Eng. Sci.* **2021**, *238*, 11. [[CrossRef](#)]
12. Almajed, A.; Tirkolaei, H.K.; Kavazanjian, E., Jr.; Hamdan, N. Enzyme Induced Biocemented Sand with High Strength at Low Carbonate Content. *Sci. Rep.* **2019**, *9*, 1–7. [[CrossRef](#)]
13. Mwandira, W.; Nakashima, K.; Kawasaki, S. Bioremediation of lead-contaminated mine waste by *Pararhodobacter* sp based on the microbially induced calcium carbonate precipitation technique and its effects on strength of coarse and fine grained sand. *Ecol. Eng.* **2017**, *109*, 57–64. [[CrossRef](#)]
14. Dilrukshi, R.A.N.; Nakashima, K.; Kawasaki, S. Soil improvement using plant-derived urease-induced calcium carbonate precipitation. *Soils Found.* **2018**, *58*, 894–910. [[CrossRef](#)]
15. Tiwari, N.; Satyam, N.; Sharma, M. Micro-mechanical performance evaluation of expansive soil biotreated with indigenous bacteria using MICP method. *Sci. Rep.* **2021**, *11*, 1–12. [[CrossRef](#)] [[PubMed](#)]
16. Xiao, J.Z.; Wei, Y.Q.; Cai, H.; Wang, Z.W.; Yang, T.; Wang, Q.H.; Wu, S.F. Microbial-Induced Carbonate Precipitation for Strengthening Soft Clay. *Adv. Mater. Sci. Eng.* **2020**, *2020*, 11. [[CrossRef](#)]
17. Ou, X.D.; Peng, Y.S.; Hou, K.W.; Su, J.; Jiang, J. Experimental research on biochemical consolidation of bauxite tailings clay. *Arab. J. Geosci.* **2019**, *12*, 10. [[CrossRef](#)]
18. Vail, M.; Zhu, C.; Tang, C.S.; Anderson, L.; Moroski, M.; Montalbo-Lomboy, M.T. Desiccation Cracking Behavior of MICP-Treated Bentonite. *Geosciences* **2019**, *9*, 16. [[CrossRef](#)]
19. Osinubi, K.J.; Eberemu, A.O.; Ijimdiya, T.S.; Yakubu, S.E.; Gadzama, E.W.; Sani, J.E.; Yohanna, P. Review of the use of microorganisms in geotechnical engineering applications. *SN Appl. Sci.* **2020**, *2*, 207. [[CrossRef](#)]
20. De Muynck, W.; Verbeken, K.; de Belie, N.; Verstraete, W. Influence of temperature on the effectiveness of a biogenic carbonate surface treatment for limestone conservation. *Appl. Microbiol. Biotechnol.* **2013**, *97*, 1335–1347. [[CrossRef](#)] [[PubMed](#)]
21. Cheng, L.; Shahin, M.A.; Chu, J. Soil bio-cementation using a new one-phase low-pH injection method. *Acta Geotech.* **2019**, *14*, 615–626. [[CrossRef](#)]
22. Gowthaman, S.; Yamamoto, M.; Nakashima, K.; Ivanov, V.; Kawasaki, S. Calcium phosphate biocement using bone meal and acid urease: An eco-friendly approach for soil improvement. *J. Clean. Prod.* **2021**, *319*, 128782. [[CrossRef](#)]
23. Gowthaman, S.; Mohsenzadeh, A.; Nakashima, K.; Kawasaki, S. Removal of ammonium by-products from the effluent of bio-cementation system through struvite precipitation. *Mater. Today Proc.* **2021**. [[CrossRef](#)]
24. Yu, X.; Zhan, Q.; Qian, C.; Ma, J.; Liang, Y. The optimal formulation of bio-carbonate and bio-magnesium phosphate cement to reduce ammonia emission. *J. Clean. Prod.* **2019**, *240*, 118156. [[CrossRef](#)]
25. Chen, L.; Song, Y.; Huang, J.; Lai, C.; Jiao, H.; Fang, H.; Zhu, J.; Song, X. Critical Review of Solidification of Sandy Soil by Microbially Induced Carbonate Precipitation (MICP). *Crystals* **2021**, *11*, 1439. [[CrossRef](#)]
26. Xiao, H.; Liu, G.; Zhang, Q.; Zheng, F.; Zhang, X.; Liu, P.; Zhang, J.; Hu, F.; Elbasit, M.A.M.A. Quantifying contributions of slaking and mechanical breakdown of soil aggregates to splash erosion for different soils from the Loess plateau of China. *Soil Tillage Res.* **2018**, *178*, 150–158. [[CrossRef](#)]
27. Wen, Y.; Yang, G.-H.; Tang, L.-S.; Xu, C.-B.; Huang, Z.-X.; Huang, Z.-M.; Zhang, Y.-C. Tests and parameters study of mechanical properties of granite residual soil in Guangzhou area. *Rock Soil Mech.* **2016**, *37*, 209–215.
28. Tang, L.-S.; Zhao, Z.-L.; Chen, H.-K.; Wu, Y.-P.; Zeng, Y.-C. Dynamic stress accumulation model of granite residual soil under cyclic loading based on small-size creep tests. *J. Cent. South Univ.* **2019**, *26*, 728–742. [[CrossRef](#)]

29. GB/T50123-2019. *Specification of Soil Test*; China Architecture and Building Press: Beijing, China, 2019. (In Chinese)
30. Luo, X.; Gao, H.; He, P.; Liu, W. Experimental investigation of dry density, initial moisture content, and temperature for granite residual soil disintegration. *Arab. J. Geosci.* **2021**, *14*, 1060. [[CrossRef](#)]
31. Li, X.-A.; Wang, L.; Yan, Y.-l.; Hong, B.; Li, L.-C. Experimental study on the disintegration of loess in the Loess Plateau of China. *Bull. Eng. Geol. Environ.* **2019**, *78*, 4907–4918. [[CrossRef](#)]
32. Liu, W.P.; Song, X.Q.; Huang, F.M.; Hu, L.N. Experimental study on the disintegration of granite residual soil under the combined influence of wetting-drying cycles and acid rain. *Geomat. Nat. Hazards Risk* **2019**, *10*, 1912–1927. [[CrossRef](#)]
33. Papadopoulos, A.; Bird, N.R.A.; Whitmore, A.P.; Mooney, S.J. Investigating the effects of organic and conventional management on soil aggregate stability using X-ray computed tomography. *Eur. J. Soil Sci.* **2009**, *60*, 360–368. [[CrossRef](#)]
34. Gowthaman, S.; Nakashima, K.; Kawasaki, S. Freeze-thaw durability and shear responses of cemented slope soil treated by microbial induced carbonate precipitation. *Soils Found.* **2020**, *60*, 840–855. [[CrossRef](#)]
35. Nafisi, A.; Montoya, B.M.; Evans, T.M. Shear Strength Envelopes of Biocemented Sands with Varying Particle Size and Cementation Level. *J. Geotech. Geoenviron. Eng.* **2020**, *146*, 04020002. [[CrossRef](#)]
36. Cardoso, R.; Pires, I.; Duarte, S.O.D.; Monteiro, G.A. Effects of clay's chemical interactions on biocementation. *Appl. Clay Sci.* **2018**, *156*, 96–103. [[CrossRef](#)]